AIMS Materials Science, 13(2): 391–409.
DOI: 10.3934/matersci.2026020
Received: 09 February 2026
Revised: 15 April 2026
Accepted: 08 May 2026
Published: 14 May 2026

https://www.aimspress.com/journal/Materials

Research article

Experimental thermal-stability evaluation of polyester/silica aerogel composites for building insulation at elevated temperature

Muhammad Zubair Farrukh[1,2,3], Muhammad Arslan[2], Zaheer Uddin Kamran[3] and Ahmed Usman Yasir[2]

[1] Mechanical and Nuclear Engineering Department, Tennessee Technological University, Cookeville, TN, 38505, USA
[2] Department of Mechanical Engineering, Faculty of Mechanical and Aeronautical Engineering, University of Engineering and Technology (UET), Taxila, 47080, Pakistan
[3] Department of Mechanical and Materials Engineering, University of Alabama at Birmingham, Birmingham, Alabama, 35294, USA

* **Correspondence:** Email: mfarrukh42@tntech.edu; Tel: +1-659-273-1069.

Abstract: Polyester-based materials are widely used in insulation systems due to their low cost and relatively low thermal conductivity; however, further reduction in heat transfer is desirable for building envelope components exposed to elevated surface temperatures. In this study, polyester–silica aerogel composite insulation tiles were fabricated and systematically evaluated to identify the filler concentration that minimizes thermal conductivity while maintaining practical curing integrity. Silica aerogel powder was incorporated into unsaturated polyester resin at 1–5 wt.% (relative to resin mass) using methyl ethyl ketone peroxide (MEKP) as the hardener and cobalt naphthenate as the accelerator, and glass-fiber reinforcement was applied as a constant layup to enhance structural integrity. Curing was performed at 120 °C. The resulting composites were characterized using Fourier transformed infrared spectroscopy (FTIR), X-ray diffraction (XRD), thermogravimetric analysis (TGA), and steady-state thermal conductivity measurement suing a guarded heat flow meter, indicating retention of the polyester chemical structure, predominantly amorphous composite formation, and improved high temperature thermal resistance with increasing silica content. The monotonic reduction in thermal conductivity was consistent with interruption of continuous matrix conduction pathways and increased thermal boundary resistance introduced by dispersed, ultra-low-conductivity aerogel domains within the polyester matrix. Thermal conductivity was measured under steady-state conditions at 55 °C using a guarded heat flow meter in triplicate (N = 3). The thermal conductivity

decreased from 0.2800 ± 0.0030 W m^{-1} K^{-1} at 1 wt.% SiO_2 to 0.2300 ± 0.0036 W m^{-1} K^{-1} at 5 wt.% SiO_2, corresponding to an overall reduction of 0.0500 W m^{-1} K^{-1} (17.9%) within the investigated range. TGA results further indicated a major decomposition event over approximately 390–500 °C, with composition-dependent residues increasing with silica loading, consistent with enhanced thermal resistance at elevated temperatures. Overall, 5 wt.% silica aerogel provides the lowest measured thermal conductivity among the tested formulations and supports the potential of these polyester-based composites for rigid insulation tile applications with practical curing feasibility for roof and building-envelope use.

Keywords: polyester composites; heat insulation tiles; polymer composites; curing behavior; low thermal conductivity composites; silica aerogel

1. Introduction

The building sector is a major energy consumer, as estimates reported in the literature indicate that 40% of worldwide energy use is associated with buildings, and energy demand is expected to increase with rising living standards and cooling needs in warm regions [1]. Roofs are a primary pathway for solar heat gain because they receive the most direct irradiation, and conventional roof surfaces can reach 65 °C, which elevates indoor temperature and increases cooling demand [2]. Therefore, lowering conductive heat transfer through the roof via effective insulation remains an important pathway to improve indoor thermal comfort and reduce reliance on active cooling systems [3,4].

Polyester resins are widely used in mechanical and electrical components and are adopted in insulation applications because of their low cost, low thermal conductivity, and high strength-to-weight ratio [5–7]. Polymeric matrix composites are widely adopted when low density, manufacturability, and property tailoring are required, and thermosetting systems remain central because curing converts the resin into a rigid, dimensionally stable network [8]. Polyester resin is repeatedly emphasized as a practical matrix because it combines low cost with favorable strength-to-weight characteristics and established composite processing routes [9]. In the composite form, polyester usually undergoes curing processing, where initiators/accelerators and temperature affect polymerization and final properties [10]. Curing is defined as a chemical/physical transformation that leads to a harder, tougher, or more stable material or linkage [11]. For unsaturated polyester, a description of the cure kinetics is complex with more than one reaction process occurring from a single point in time [12]. The mechanism is usually illustrated by the steps of initiation, propagation, and termination. The decomposition of the initiator produces free radicals, and the radicals are used to react with the styrene or polyester in polymerization [13]. The above cited literature emphasizes that the key parameters that govern curing include not only temperature and pressure but also concentration of hardener/initiator, accelerator, resin, filler, and reinforcement [14]. Consequently, conductivity reduction strategies must be assessed as coupled formulation/process problems, otherwise the system may cascade into incomplete curing, void formation, or property scatter conditions that compromise performance and reproducibility. Epoxy resins can offer high mechanical performance and attractive chemical behavior in several structural situations. The processing challenges are mentioned repeatedly: Smooth surfaced epoxy composites are sometimes hard to achieve because of the adhesive behavior; in addition, the

formation of cracks and bubbles in the curing process is characterized as a significant issue [15]. Vinyl ester resins are said to possess curing properties and chemical properties similar to polyester and may have a better mechanical and corrosion performance, but polyester is desired due to its lower thermal conductivity and the short life of vinyl ester [16]. Phenolic resins are referenced for low smoke and flammability properties and may have low thermal conductivity at a low price [17]. Collectively, these comparisons support taking a pragmatic approach: The research need is not simply to switch matrices but to engineer polyester-based composites toward lower thermal conductivity with equal or better cure stability and fabrication practicality. Within polyester systems, the cited literature identifies common curing agents and practical processing considerations. Methyl ethyl ketone peroxide (MEKP) is widely used as an initiator/hardener and cobalt naphthenate as an accelerator in polyester composite curing [18,19]. The same literature warns that non-optimal concentrations may increase radical generation in ways that affect curing and the properties of the final composite [20]. This constraint is particularly important for filler-enhanced insulation composites because the temptation to increase filler content for lower conductivity must be balanced against the risk of shifting the system into a curing regime that yields unstable networks or defect-prone microstructures. Therefore, when insulation performance is targeted, the formulation must be designed so that thermal conductivity reduction and cure integrity are optimized rather than traded off. Reinforcement is generally introduced to ensure structural integrity and shape formation rather than to directly minimize thermal conductivity.

Fiber reinforcement is described as enabling specific shape and structure development for desired products [21]. In polymer composites, reinforcement such as glass fiber is frequently used to develop structural integrity while maintaining insulation performance; glass fiber is attractive due to low cost and good mechanical, chemical, and electrical insulation properties [22,23]. In contrast, carbon fiber is defined as high-strength, high-stiffness reinforcement with tolerance to high temperature, which is accompanied by high expenses and galvanic corrosion potential, which has caused the preference of glass fiber for many composite systems. Kevlar fibers are mentioned as light and tough with high impact resistance but weakened by their weakness in compression and machining difficulties [24]. Boron fiber is said to have high stiffness and strength but is expensive and restricted for complex shapes and is difficult to handle [25]. Ceramic composites, particularly oxide based ceramic composites, are stated to be suited for very high temperature use and not suitable for heat insulation in this regard [26]. Among insulating fillers, silica (SiO_2) aerogel is known as one of the most effective insulating solids with very low thermal conductivity and light density owing to its less porous structure and high surface area [27,28]. Aerogels have been mentioned in widespread application areas such as insulated buildings, appliances, automobiles, and solar devices as well as in physical forms such as monolith, granules, and powders [29–31]. For polymer composite integration, powders are of particular interest as they can be integrated into the resin before curing and may offer the possibility of wide distribution of an ultra-low conductivity phase in the polymer network. Nevertheless, silica aerogels are typically brittle with low mechanical strength and, for this reason, can be more practically used by embedding them into composite systems to extend usability in real structures [32]. In effect, silica aerogel has insulation potential, but the composite architecture (dispersion quality, filler loading, interfacial compatibility, and cure stability) determines whether this potential is realized in a durable tile.

Due to the dual needs for thermal and structural performance of insulation composites, the above cited literature supports multi-technique validation of composite integrity, rather than relying on just one thermal measure. Characterization tools, including X-ray diffraction (XRD), differential scanning

calorimetry (DSC), Fourier-transform infrared spectroscopy (FTIR), and thermogravimetric analysis (TGA) are mentioned as typical methods to check the composition, the curing quality, and the thermal degradation behavior of polymer composites [33]. Accordingly, an insulation composite intended for tile applications benefits from a combined reporting strategy that includes thermal conductivity trends supported by chemical and structural verification that the composite is properly formed and thermally stable. Reliable thermal conductivity measurement is central for screening insulation materials. Thermal conductivity methods are classified into steady-state and transient approaches [34,35]. Steady-state methods are emphasized as efficient for low thermal conductivity materials and composites, albeit with longer test times and larger specimen requirements [36]. Guarded hot plate is identified as a highly accurate approach for insulating materials and composites [37], and guarded heat flow meter methods are described as widely used for low-conductivity materials, relying on heat-flux sensing and Fourier's law to infer conductivity [38,39]. Transient methods offer faster tests but are described as less accurate in some contexts due to sensitivity to uncertainties in properties such as specific heat capacity and density [40].

Although polyester-silica and polyester-silica aerogel composites were explored in the context of thermal insulation, the literature primarily presents thermal conductivity at ambient or nearly ambient temperatures and frequently considers curing behavior, structural characterization, and thermal stability as independent constructs, but not as a unified approach to material selection. Specifically, the literature regarding the systematic assessment of the relationship between curing conditions and chemical integrity, structural evolution, behavior at high temperatures, and service-relevant thermal conductivity is scarce. The originality of this research is the creation of a single structure-processing-property evaluation of polyester-silica aerogel composites (1–5 wt.% SiO_2) under a regulated curing environment (120 °C) where FTIR, XRD, TGA, and steady-state thermal are conducted. Moreover, in stark contrast to researchers who concentrate on individual properties, we directly correlate curing integrity to thermo-physical performance to find practically viable insulation formulations. Our major aims in this research are: (i) to demonstrate the curing stability of polyester silica aerogel composites under controlled processing conditions; (ii) to experimentally verify the maintenance of polymer chemistry and the predominantly amorphous structure at different silica loadings; (iii) to measure thermal stability and degradation behavior up to 600 °C; and (iv) to determine the optimal silica aerogel loading (5 wt.%). These results provide a realistic foundation for the development of polyester-based thermal insulating tiles that offer improved thermal performance and manufacturability.

2. Materials and methods

2.1. Curing process of polyester/silica aerogel composites

Unsaturated polyester resin was used as the matrix material, silica aerogel powder as the insulating filler, MEKP as the initiator/hardener, and cobalt naphthenate (CN) as the curing accelerator. Silica aerogel particles used in this study were purchased from a commercial supplier (CABOT Corporation USA), which is widely used for thermal insulation applications. Preliminary curing trials were conducted by heating the formulated resin system on a hot plate over a temperature range of 40–160 °C to identify a defect-free curing window and to minimize bubble formation. During these trials, surface temperature was recorded at 5 min intervals, and visual observations of gelation, surface smoothness, and void/bubble formation were used to assess curing quality. For the composite

specimens reported in this study, curing was carried out on a hot plate maintained at 120 °C, and the surface temperature evolution was recorded at 1 min intervals under ambient starting temperatures (Ts = 18–27 °C), as provided in Tables S1–S5 in Supplementary Information. The overall experimental procedure, including composite fabrication, curing, and thermo-physical characterization workflow, is schematically illustrated in Figure 1. Representative fabricated samples and the hot plate curing setup used for composite preparation are shown in Figure 2, highlighting the processing conditions and specimen configurations.

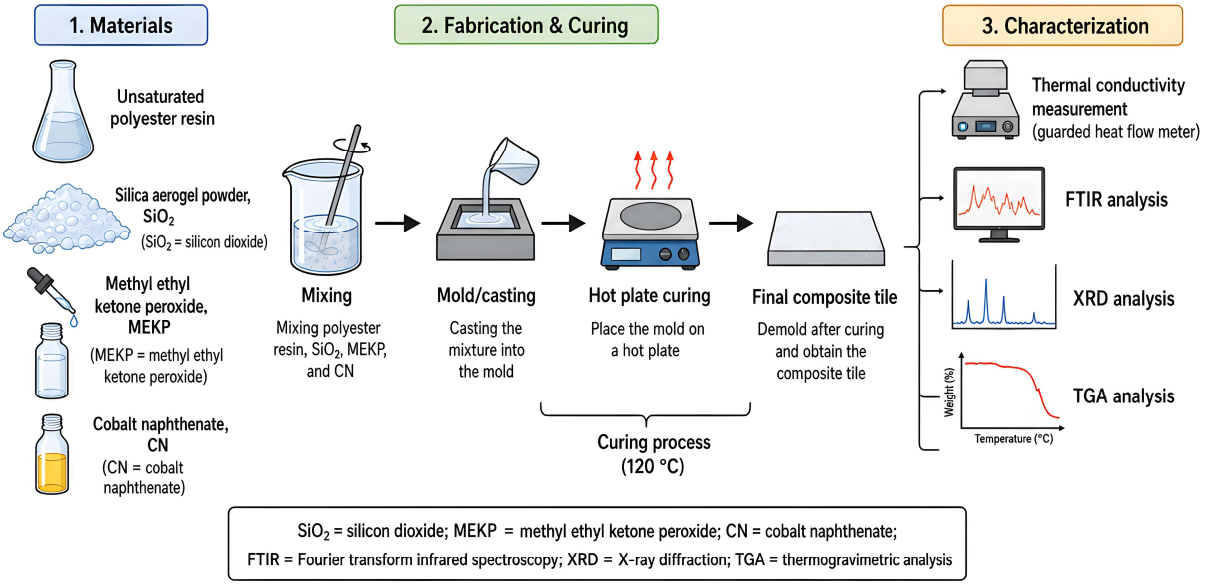

Figure 1. Schematic of fabrication, curing, and thermo-physical characterization workflow for polyester–silica aerogel composites.

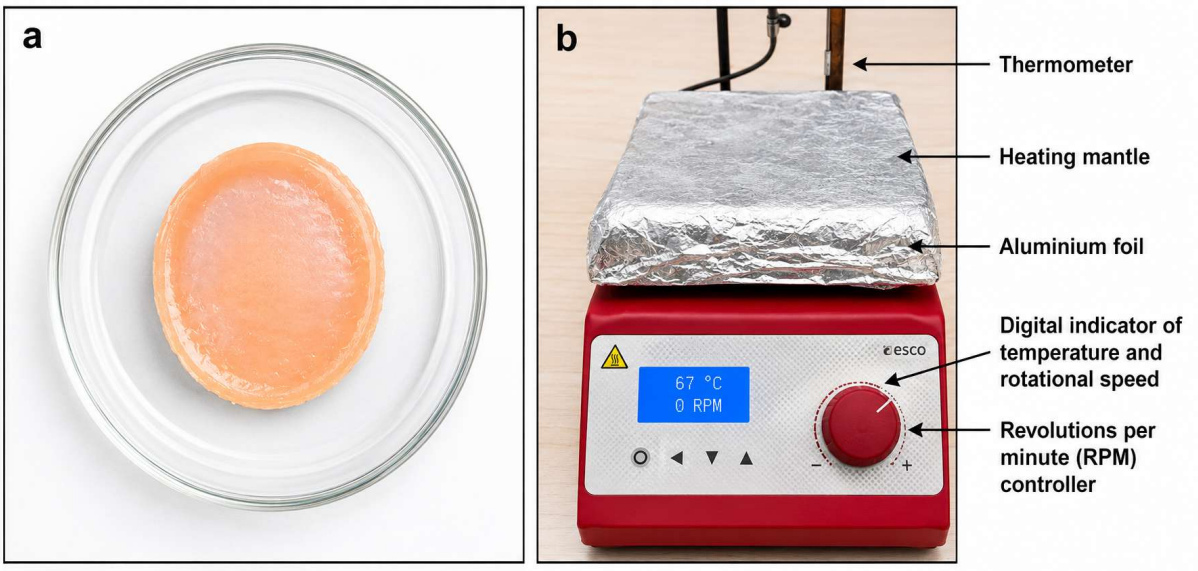

Figure 2. Samples prepared: (a) polyester sample; (b) hot plate setup of polyester/silica aerogel curing.

Bubble/void formation was primarily associated with off-stoichiometric dosing and inadequate mixing of the initiator (MEKP) and accelerator (CN). Therefore, MEKP and CN were added in small, controlled quantities and mixed thoroughly to ensure uniform polymerization and a smooth cured surface. Based on preliminary trials, a curing temperature of 120 °C provided the best compromise between rapid curing and surface quality for the polyester/silica aerogel formulations; this temperature was maintained until complete solidification. All constituents (polyester resin, silica aerogel, MEKP, and CN) were commercially available and were used without any additional pre-treatment. Composite batches were prepared at a fixed polyester resin mass of 15 g per batch, while silica aerogel loading was varied from 1–5 wt.% relative to the polyester resin mass (0.15, 0.30, 0.45, 0.60, and 0.75 g for 1–5 wt.%, respectively). The selected silica aerogel loading range (1–5 wt.%) was based on preliminary trials and practical processing constraints. Very low loadings (<1 wt.%) were expected to produce negligible changes in thermal behavior, whereas higher loadings (>5 wt.%) were found to increase the likelihood of particle agglomeration, non-uniform dispersion, and curing defects such as void formation and surface irregularities. In addition, excessive filler content can interfere with the polymerization process by altering the effective resin-to-hardener interaction. Therefore, the selected range provides a balance to systematically investigate the influence of silica aerogel on composite performance while ensuring consistent curing quality and structural integrity. MEKP and CN were dosed at approximately 0.07 g and 0.04–0.05 g per batch, respectively, and kept approximately constant across batches to enable a direct comparison of curing behavior and subsequent property measurements. The detailed batch compositions and representative curing-temperature traces are summarized in Tables S1–S5.

2.2. Sample preparation

The composite tiles were fabricated as square panels with dimensions of 5 in × 5 in × 0.5 in. Five formulations were prepared using unsaturated polyester resin (15 g per batch), glass-fiber reinforcement, MEKP (0.07 g) as the hardener, and cobalt naphthenate (0.04–0.05 g) as the accelerator. Silica aerogel loading was defined relative to the polyester mass (15 g), yielding silica masses of 0.15 g (1 wt.%), 0.30 g (2 wt.%), 0.45 g (3 wt.%), 0.60 g (4 wt.%), and 0.75 g (5 wt.%) (Tables S1–S5). For each batch, the polyester resin was first mixed with the required silica mass according to the target formulation, followed by the addition of cobalt naphthenate and MEKP. The mixture was then stirred for a fixed duration until no visible agglomerates remained before casting into the prepared mold. Glass-fiber reinforcement was applied as a constant layup across all formulations. Although glass fiber had a higher intrinsic thermal conductivity than the polyester matrix, its configuration and quantity was uniform across all samples; therefore, its contribution to overall heat transfer was consistent and did not influence the comparative assessment of silica aerogel loading. Tables S1–S5 report the resin-side formulation (polyester, silica aerogel, initiator, and accelerator), while the reinforcement configuration was held unchanged to ensure that comparative trends reflected silica loading. Curing was carried out on a hot plate maintained at 120 °C, and the surface temperature evolution was recorded at 1 min intervals under ambient starting temperatures (Ts = 18–27 °C, Tables S1–S5). The exothermic curing response showed rapid surface-temperature increases to peak values of approximately 94 °C (1 wt.%), 97 °C (2 wt.%), 102 °C (3 wt.%), 93 °C (4 wt.%), and 109 °C (5 wt.%), followed by a progressive decline toward approximately 61–77 °C within the recorded curing window. A mold cover was used during curing to minimize exposure to reactive constituents. After curing, the tiles were

demolded and immediately dipped in water to dissipate residual heat, as excessive thermal loading was observed to promote crack formation. Finally, the tiles were dried under ambient conditions and inspected for macroscopic defects (cracking, warpage, and visible voids) prior to characterization. The final fabricated composite tiles with varying silica aerogel loadings (1–5 wt.%) are presented in Figure 3, illustrating the surface quality and physical integrity of the cured samples.

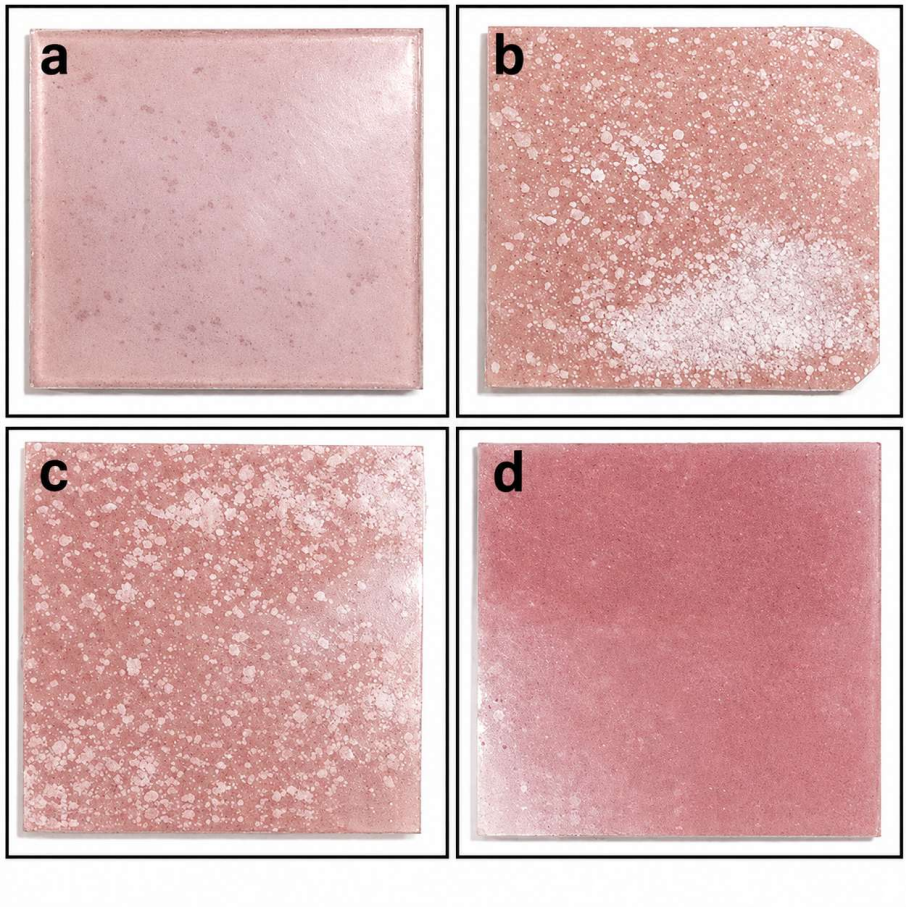

Figure 3. Final product: (a) polyester tile; (b) 1% silica tile; (c) 3% silica tile; and (d) 5% silica tile.

2.3. Characterization of cured polyester composite

Powder XRD was used to examine the structural characteristics of the cured polyester/silica aerogel composites. XRD patterns of the fabricated samples were obtained using a PANalytical X'Pert diffractometer and analyzed using HighScore Plus software. Measurements were performed using Cu-Kα radiation with a wavelength λ of 0.15406 nm, and phase screening was performed by comparison with reference patterns from the ICDD/PDF database. The diffraction condition followed Bragg's law (Eq 1):

$$n\lambda = 2dsin\theta \tag{1}$$

where n is the diffraction order, λ is the X-ray wavelength, d is the interplanar spacing (d-spacing), and θ is the Bragg angle. FTIR spectroscopy was used to identify functional groups and assess the chemical features of the cured composites. All samples were analyzed using a JASCO FTIR

spectrometer over the wavenumber range of 400–4000 cm^{-1}, and the spectra were used to examine characteristic absorption bands of the polyester matrix and changes associated with silica aerogel incorporation. TGA was performed using a Hi-Res TGA 2950 (TA Instruments) to evaluate the thermal stability and degradation behavior of the cured materials. The measurements were conducted under air flow (74 mL/min) at a heating rate of 20 °C/min, and mass-loss profiles were recorded as a function of temperature. Thermal conductivity (k) was measured at 55 °C using a guarded heat flow meter (DTC-300) in accordance with the steady-state guarded method (ASTM E1530). This steady-state approach was well suited for low-conductivity materials and provided a consistent basis for comparing formulation-dependent changes in composite thermal performance. The elevated test temperature (55 °C) was selected to represent service-relevant roof/tile thermal exposure rather than relying solely on ambient-condition measurements. Prior to testing, specimen thickness was measured using a vernier caliper, and the measured thickness was used in the ASTM E1530 conductivity calculation; measurements were recorded only after the instrument output indicated steady-state stabilization (i.e., negligible drift in heat-flow response and temperature gradient at the setpoint). The instrument operating range was 0.1–40 W m^{-1} K^{-1}. Thermal conductivity measurements were repeated three times (N = 3) for each formulation under identical test conditions, and the reported values represent the mean ± standard deviation (SD). Accordingly, the measured thermal conductivity values were 0.2800 ± 0.003 (1 wt.% SiO_2), 0.2647 ± 0.0050 (2 wt.% SiO_2), 0.2540 ± 0.0036 (3 wt.% SiO_2), 0.2367 ± 0.0035 (4 wt.% SiO_2), and 0.2300 ± 0.0036 W m^{-1} K^{-1} (5 wt.% SiO_2). The measured thermal conductivity values for all composite formulations at 55 °C are summarized in Table 1, including the mean values and associated standard deviations. The accuracy and operating ranges of the instruments used for characterization are listed in Table 2.

Table 1. Thermal conductivity of polyester–silica aerogel composites at 55 °C as a function of SiO_2 loading (mean ± SD, N = 3).

SiO_2 loading (wt.%)	N	Mean k (W m^{-1} K^{-1})	SD (W m^{-1} K^{-1})
1	3	0.2800	0.0030
2	3	0.2647	0.0050
3	3	0.2540	0.0036
4	3	0.2367	0.0035
5	3	0.2300	0.0036

Table 2. Accuracy and operating range of measuring instruments used in the experimental setup.

Instrument	Model	Accuracy	Operating range
XRD	PANalytical X'Pert	Angular accuracy: ±0.0025°	2θ: −40° to 160°
FTIR	JASCO FT-IR spectrometer	Wavenumber accuracy: ±0.01 cm^{-1}	400–4000 cm^{-1}
TGA	Hi-Res TGA 2950 (TA Instruments)	Balance accuracy: ±0.1%	Ambient to 1000 °C
k	DTC-300	Accuracy: ±3%	−20 to 300 °C; 0.1–40 W m^{-1} K^{-1}

Table 3 consolidates composition, curing parameters, and thermo-physical properties of the polyester–silica aerogel composites. All samples were cured at 120 °C, isolating the effect of silica loading (1–5 wt.%). Increasing SiO_2 content increased peak exothermic curing temperature and high-temperature residue, indicating enhanced thermal persistence, while the primary degradation range of the polyester matrix remained unchanged (≈390–500 °C). Thermal conductivity at 55 °C decreased monotonically from 0.2800 ± 0.0030 to 0.2300 ± 0.0036 W m^{-1} K^{-1} with increasing silica content. Among the investigated formulations, 5 wt.% SiO_2 exhibited the optimal balance of curing behavior, thermal stability, and insulation performance. The selection of characterization techniques in this study was guided by the need to establish a direct linkage between material structure and thermal performance. FTIR was employed to confirm the chemical integrity of the polyester matrix and to assess any changes associated with the silica aerogel incorporation. XRD was used to evaluate the structural nature of the composites, particularly to verify the predominantly amorphous character, which influenced heat conduction behavior. TGA was selected to quantify the thermal stability and degradation characteristics at elevated temperatures, providing insight into high-temperature performance and residual inorganic content. Finally, steady state thermal conductivity was conducted directly to assess insulation performance under relevant conditions. Together, these techniques provide a framework to evaluate structure-property relationships in developed countries.

Table 3. Summary of polyester–silica aerogel composite formulations, curing conditions, and thermo-physical characterization results.

Sample	SiO_2 (wt.%)	SiO_2 (g)	Polyester (g)	MEKP (g)	CN (g)	Cure (°C)	Ts (°C)	Peak surface T (°C)	Main TGA loss (°C)	Residue at 600 °C (%)	k at 55 °C (W m^{-1} K^{-1})
P–SA1	1	0.15	15	0.07	=0.04–0.05	120	18–27	94	390–500	11–12	0.2800 ± 0.0030
P–SA2	2	0.30	15	0.07	=0.04–0.05	120	18–27	97	390–500	12–13	0.2647 ± 0.0050
P–SA3	3	0.45	15	0.07	=0.04–0.05	120	18–27	102	390–500	15–16	0.2540 ± 0.0036
P–SA4	4	0.60	15	0.07	0.05	120	20	93	390–500	17–18	0.2367 ± 0.0035
P–SA5	5	0.75	15	0.07	0.04	120	18	109	390–500	19–20	0.2300 ± 0.0036

3. Results

3.1. Characterization

3.1.1. FTIR

FTIR spectra of the polyester and silica aerogel composites cured at 120 °C are compared in Figure 4 for silica loadings of 1–5 wt.% and show a consistent polyester fingerprint with superimposed silica-related features. All spectra exhibit a broad O–H stretching band at approximately 3426–3461 cm^{-1} (e.g., 3426 cm^{-1} for 1 wt.% and 3461 cm^{-1} for 5 wt.%), consistent with hydroxyl-containing surface species associated with silica (silanol groups) and/or weakly bound moisture; the breadth of this band reflects hydrogen-bonded and surface-associated O–H groups rather than a single discrete vibrational mode. The cured polyester network is evidenced by the ester carbonyl (C=O) absorption in the 1710–1734 cm^{-1} region, appearing at 1712 (1 wt.%), 1712 (2 wt.%), 1734 (3 wt.%), 1725 (4 wt.%), and 1710 cm^{-1} (5 wt.%). Minor variations in the apparent carbonyl peak position and shape can arise from changes in the local chemical environment (e.g., polarity and proximity to hydrogen-bonding sites) and/or spectral overlap and processing and are not indicative of the formation of new functional groups. Consistent with this observation, no new diagnostic absorption bands attributable to chemical modification of the polyester backbone are detected upon aerogel addition, indicating that silica incorporation does not alter the primary polyester chemistry. Aliphatic C–H stretching bands are present in the 2827–2935 cm^{-1} region (e.g., 2827 cm^{-1} for 3 wt.% and 2859–2935 cm^{-1} for higher loadings), reflecting CH_2/CH_3 vibrations of the cured polymer network. The C–O–C/C–O stretching region also remains evident across all compositions, with bands between approximately 1224 and 1353 cm^{-1} (1353 cm^{-1} for 1 wt.%, 1257 cm^{-1} for 2 wt.%, 1267 cm^{-1} for 3 wt.%, 1275 cm^{-1} for 4 wt.%, and 1224 cm^{-1} for 5 wt.%), confirming retention of ester and ether linkages after curing. In the lower-wavenumber region, features around 933–950 cm^{-1} (1–4 wt.%) and a more distinct band near 817 cm^{-1} (5 wt.%) are consistent with silicate-related vibrations (Si–O and Si–O–Si modes) contributed by the silica-containing phase. With increasing SiO_2 loading, the relative visibility of silicate-associated bands increases as a larger fraction of the composite response originates from Si–O vibrations and overlap with polymer bands becomes less dominant. Weak features near 2395–2418 cm^{-1} should be interpreted cautiously, as this region can be influenced by atmospheric background contributions such as CO_2 absorption in FTIR measurements. Overall, the persistence of the polyester carbonyl and C–O–C/C–O bands across 1–5 wt.% demonstrates that curing at 120 °C preserves the characteristic polyester chemistry, while the gradual evolution of silicate-associated features reflects increasing silica contribution and polymer–filler interfacial proximity rather than the formation of new chemical phases. Thus, FTIR confirms successful curing of the polyester network across all formulations, with silica aerogel incorporation primarily influencing spectral intensity and local environments through physical dispersion and interfacial effects.

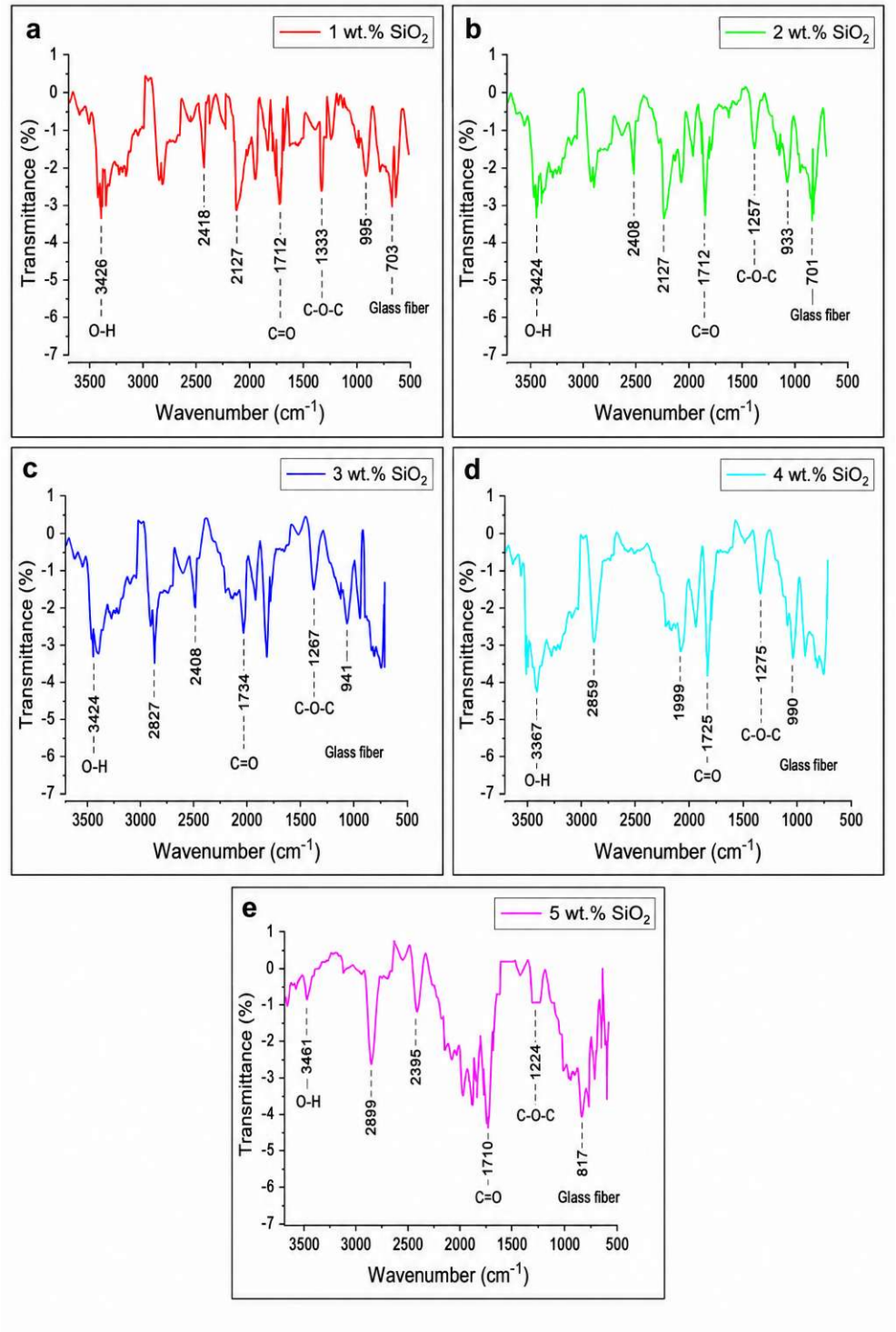

Figure 4. FTIR analysis of SiO_2 concentrations: (a) 1 wt.%; (b) 2 wt.%; (c) 3 wt.%; (d) 4 wt.%; and (e) 5 wt.%.

3.1.2. XRD

XRD patterns of polyester/silica aerogel composites containing 1–5 wt.% SiO_2 are presented in Figure 5 to evaluate their structural characteristics. Across all compositions, the diffractograms are dominated by a broad diffuse background with only weak superimposed features, indicating that the composites are predominantly amorphous. This response is physically expected because Bragg

diffraction requires long-range periodic atomic order; cured unsaturated polyester is largely non-crystalline (crosslinked network) and silica aerogel is typically amorphous, so the scattering intensity is distributed as a wide "halo" rather than concentrated into sharp reflections. Superimposed on this amorphous background, a limited number of low-intensity features appear around $2\theta \approx 18–25°$, 28–34°, and 59–63°. These features are best interpreted as minor silica/silicate-related contributions or short-range ordering effects associated with the composite constituents that are present as trace ordered domains or short-range correlations. Moreover, because their intensities are weak and do not form a consistent, strong peak set, they do not indicate the formation of a new crystalline phase in the polymer matrix. Importantly, increasing silica loading from 1 to 5 wt.% does not produce the appearance of new sharp peaks or a systematic growth of existing peaks; instead, the overall pattern shape remains similar, implying that silica aerogel functions primarily as a dispersed, low-crystallinity filler, with no evidence of silica-induced crystallization within the investigated range. Therefore, the XRD results support the conclusion that the fabricated composites remain amorphous dominated across the investigated silica range, with only weak reflections attributable to minor silica/silicate contributions rather than crystallization of the polyester matrix. The predominantly amorphous structure is favorable for thermal insulation, as the absence of long-range order suppresses phonon transport and is consistent with the observed reduction in thermal conductivity.

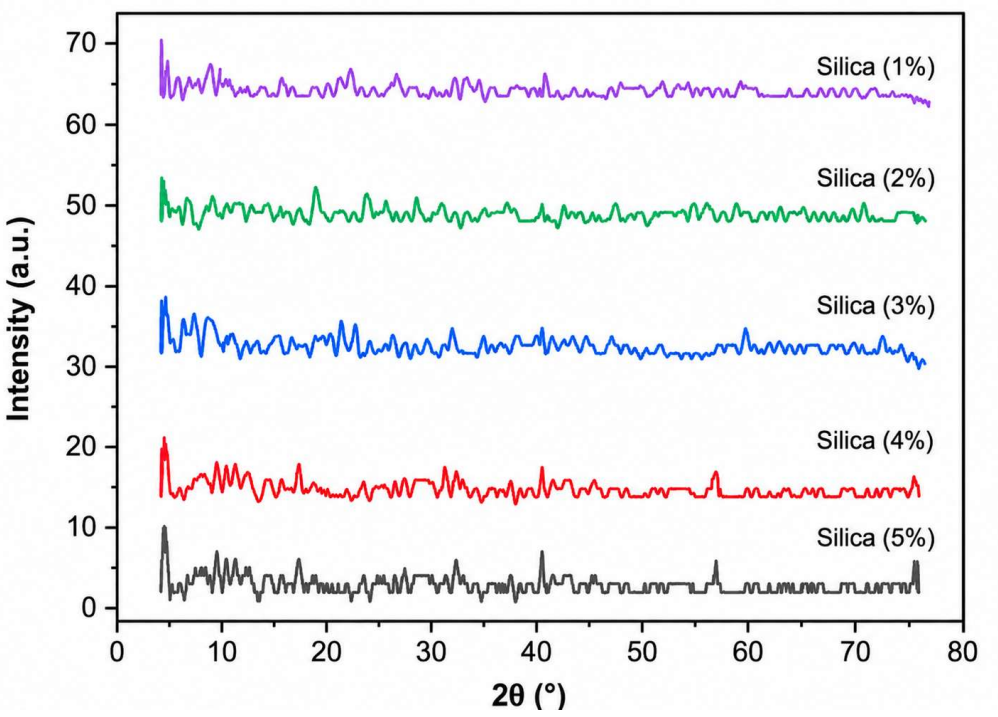

Figure 5. XRD patterns of polyester/silica aerogel composites containing 1–5 wt.% SiO_2, showing predominantly amorphous behavior with no evidence of silica-induced crystallization.

The structural characterization results provide direct insights into the observed thermal conductivity reduction. The increasing presence of silicate-associated bands in the FTIR spectra with higher SiO_2 loadings confirms the progressive incorporation and dispersion of silica aerogel within the polyester matrix, which increases the number of polymer-filler interfaces. These interfaces act as thermal resistance sites, impeding heat flow across the composite. Concurrently, the XRD results indicate that all composites remain predominantly amorphous, with no evidence of silica-induced

crystallization. The absence of long-range ordered structures suppresses phonon transport, further limiting heat conduction. Together, these features support a mechanism in which dispersed aerogel domains interrupt continuous conduction pathways and increase heat-flow, resulting in the observed decrease in thermal conductivity with increasing silica content.

3.1.3. TGA

Figure 6 presents the TGA profiles of polyester composites containing 1–5 wt.% silica aerogel, plotted as mass remaining (weight %) versus temperature. In TGA measurements, the recorded weight decreases with increasing temperature due to progressive mass loss, initially through removal of physically held species such as trace moisture and low-molecular-weight components, and subsequently through chemical degradation of the polymer network into volatile products that leave the sample pan. In these results, all formulations remain comparatively stable up to approximately 350–380 °C, indicating that low-temperature mass loss is limited, and that the composites do not undergo substantial degradation prior to this range. A major mass-loss step is observed between approximately 390 and 500 °C, where the curves drop steeply, corresponding to the primary thermal and oxidative decomposition of the unsaturated polyester matrix. Within this temperature interval, oxidative reactions are associated with the formation of peroxide-type intermediates at susceptible sites in the polymer backbone, followed by chain scission and rapid evolution of volatile degradation products, which results in a sharp decrease in the remaining mass. Beyond 500 °C, the curves transition into a slower tailing region between 500 and 600 °C as decomposition gradually diminishes and the system approaches its final residue. Importantly, the residual mass at 600 °C increases systematically with silica loading, reaching approximately 11%–12% (1 wt.%), 12%–13% (2 wt.%), 15%–16% (3 wt.%), 17%–18% (4 wt.%), and 19%–20% (5 wt.%), reflecting the increasing proportion of the thermally stable inorganic silica phase that does not volatilize within this temperature range. Higher silica contents also contribute to the formation of a more persistent residue or char–silica barrier, which can hinder heat transfer and volatile diffusion during the later stages of degradation. The 1 wt.% composite exhibits the most polymer-dominated behavior, resulting in the lowest final residue and a comparatively sharper mass reduction during the main decomposition step, whereas composites with higher silica loadings retain greater residual mass due to the increased non-combustible silica fraction and the associated barrier effect.

Overall, Figure 6 indicates that although the principal decomposition window of the polyester matrix remains similar across the 1–5 wt.% silica aerogel range (390–500 °C), increasing silica content enhances the high-temperature residue and improves the apparent thermal persistence of the composites up to 600 °C. Because Figure 6 is presented as TGA mass remaining (weight, %) versus temperature, the discussion focuses on the temperature ranges of major mass loss and the final residue at 600 °C, which can be directly interpreted from the curves. A detailed kinetic assessment, such as determination of maximum mass-loss rates and characteristic degradation temperatures, would require derivative thermogravimetric (DTG) analysis and is therefore suggested for future work.

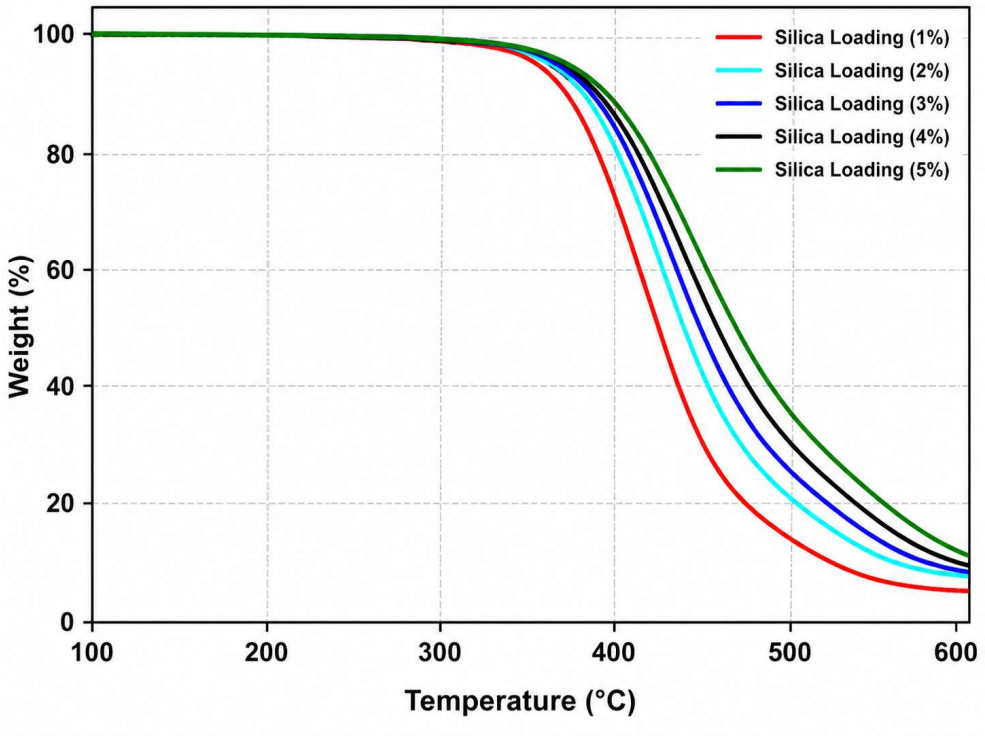

Figure 6. TGA of different concentrations of silica with polyester.

To provide a quantitative assessment of thermal stability, key thermogravimetric parameters are summarized in Table 4.

Table 4. Quantitative assessment of thermal stability, key thermogravimetric parameters.

Sample	SiO_2 (wt.%)	Temperature at 5% mass loss (Td,5%, °C)	Maximum degradation temperature (Tmax, °C)	Residue at 600 °C
P-SA1	1	365	425	11–12
P-SA2	2	370	430	12–13
P-SA3	3	375	435	15–16
P-SA4	4	380	440	17–18
P-SA5	5	385	445	19–20

The results indicate that while Td,5% and Tmax remain within a similar range across all formulations, consistent with the dominant polyester matrix, the residual mass increases systematically with silica aerogel content, confirming enhanced thermal persistence due to the increasing inorganic fraction and associated barrier effects.

3.2. Thermal conductivity

At a test temperature of 55 °C (328.15 K), the k, of the polyester/silica aerogel composites decreases systematically with increasing SiO_2 loading (Figure 7), from 0.2800 ± 0.0030 (1 wt.%) to 0.2647 ± 0.0050 (2 wt.%), 0.2540 ± 0.0036 (3 wt.%), and 0.2367 ± 0.0035 W m^{-1} K^{-1} (4 wt.%), reaching a minimum of 0.2300 ± 0.0036 W m^{-1} K^{-1} (5 wt.%). Thermal conductivity measurements were repeated three times (N = 3) for each formulation, and values are reported as mean ± SD. It is important to note that although silica aerogel exhibits ultra-low intrinsic thermal conductivity, the

relatively high composite thermal conductivity values observed in this study are attributed to low filler loading (1–5 wt.%), where the polyester matrix remains the dominant continuous phase for heat conduction. Due to the low density of aerogel, the corresponding volume fraction remains limited, resulting in a polymer-dominated heat transfer pathway. Therefore, the observed reduction (~17.9%) is consistent with effective medium behavior for dispersed insulating inclusions. From a practical standpoint, these composites are designed as rigid insulation tiles rather than ultra-low-conductivity materials, offering a balance between thermal performance, structural stability, and manufacturability for building-envelope applications such as roofing and wall insulation panels. Overall, increasing silica aerogel content from 1 to 5 wt.% reduces k by 0.0500 W m^{-1} K^{-1} (17.9%), indicating progressively improved insulation performance within the investigated range. This monotonic decrease is consistent with expected composite heat-transfer behavior. Furthermore, silica aerogel is an ultra-low-conductivity phase because its nanostructured, highly porous network limits solid-state heat transport through reduced solid connectivity and promotes heat flow through thin ligaments and gas-filled pores. When dispersed within a higher-conductivity polyester matrix, aerogel domains act as distributed thermal resistance regions. As the aerogel fraction increases from 1 to 5 wt.%, two effects become more pronounced: (i) disruption of continuous matrix conduction pathways, which increases effective heat-flow tortuosity; and (ii) increased interfacial thermal resistance, because polymer–aerogel interfaces introduce additional thermal boundary resistance, and their number increases with filler loading. The relatively larger reduction observed between 1 and 2 wt.% (0.2800 to 0.2647 W m^{-1} K^{-1}) is consistent with the onset of effective barrier formation at low filler content, where a modest increase in aerogel fraction can significantly disrupt the most continuous heat-conduction paths. At higher loadings, further decreases (e.g., 0.2540 to 0.2367 W m^{-1} K^{-1} between 3 and 4 wt.%) remain consistent with an increasing frequency of low-k regions and interfaces encountered by the heat flux as filler content rises. Under identical steady-state test conditions at 55 °C, the 5 wt.% composite exhibits the lowest measured k and therefore provides the highest insulation performance among the tested compositions.

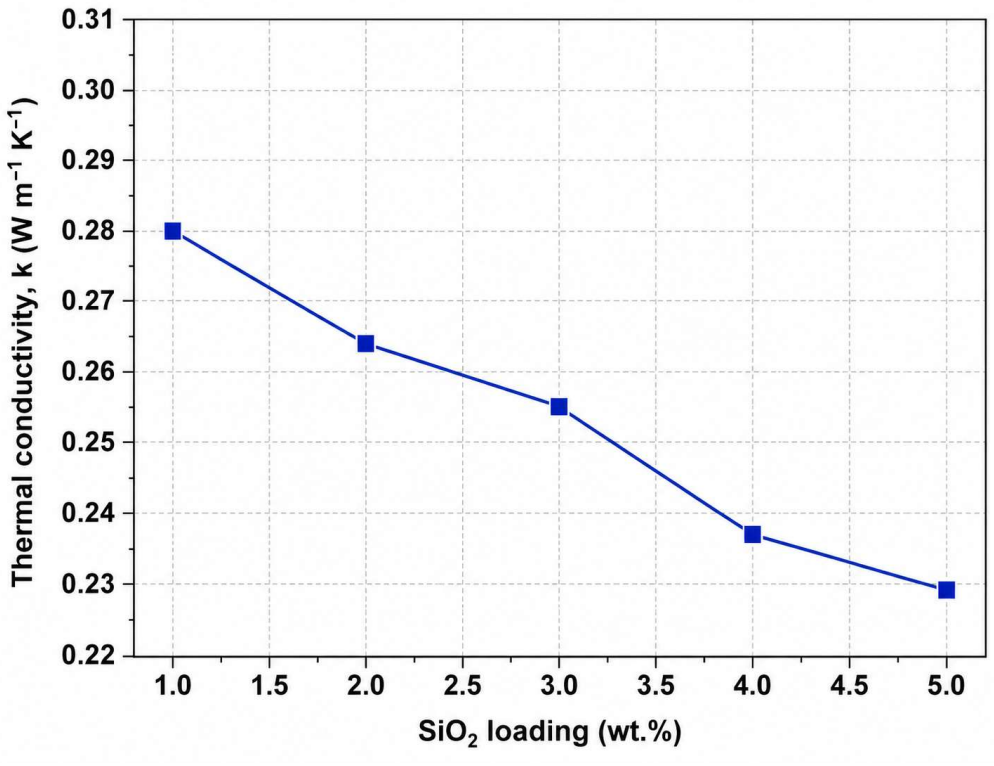

Figure 7. Thermal conductivity of different concentrations of silica with polyester.

Since the glass-fiber reinforcement is identical in all formulations, its contribution to effective thermal conductivity is uniform across all samples. Therefore, the observed variations in thermal conductivity are attributed to changes in silica aerogel loading rather than reinforcement effects. The dependence of thermal conductivity on silica aerogel loading is illustrated in Figure 7, where a monotonic decrease in k is observed with increasing SiO_2 content, confirming the effectiveness of aerogel incorporation in enhancing insulation performance.

4. Conclusions

In this work, we demonstrate that silica aerogel can be incorporated into an unsaturated polyester matrix to produce insulation tiles with stable curing at 120 °C and a consistent improvement in thermal performance at elevated temperature. Across 1–5 wt.% SiO_2, spectroscopy and diffraction results indicate that the polyester network is retained, and the composites remain predominantly amorphous, while thermogravimetric behavior shows increased inorganic residue with higher aerogel content. Most importantly, the thermal conductivity measured at 55 °C decreases monotonically with silica loading, identifying an optimal formulation within the investigated range.

- Polyester–silica aerogel tiles (1–5 wt.% SiO_2) are fabricated successfully under a consistent curing protocol at 120 °C.
- FTIR and XRD confirm retention of the polyester fingerprint and a predominantly amorphous composite structure across all formulations.
- TGA indicates comparable main degradation behavior, with increasing residue as SiO_2 loading increases.
- At 55 °C, the k decreases monotonically from 0.2800 ± 0.0030 to 0.2300 ± 0.0036 W m^{-1} K^{-1} (1–5 wt.% SiO_2; N = 3), corresponding to a 17.9% reduction.
- Within 1–5 wt.% SiO_2, 5 wt.% provides the lowest measured thermal conductivity and is the best-performing composition among those tested.

5. Future recommendations

Although this experiment determines the thermal and thermo-chemical functionality of polyester-silica aerogel composites, additional research is needed to justify their application in the building-envelope contexts. The mechanical properties (e.g., flexural strength, impact resistance, and dimensional stability) should be thoroughly evaluated in future to indicate structural reliability in the service conditions. Moreover, long term durability tests in environmental ageing conditions, including thermal cycling, moisture exposure, and ultraviolet (UV) radiation, need to be conducted to determine the performance degradation with time. For an application perspective, scalability and manufacturability issues such as large-area fabrication, cost optimization, and compatibility with roofing and wall systems should also be explored. These guidelines will assist in closing the gap between laboratory-scale material development and practice.

Use of AI tools declaration

The authors declare they have not used Artificial Intelligence (AI) tools in the creation of this article.

Acknowledgments

This research received no external funding.

Author contributions

Muhammad Zubair Farrukh: conceptualization, methodology, formal analysis, software, writing—review & editing, and resources; Muhammad Arslan: formal analysis, investigation, validation, data curation, writing—original draft, writing—review & editing; Zaheer Uddin Kamran: formal analysis, methodology, writing—review & editing; Ahmed Usman Yasir: conceptualization, investigation, validation, data curation.

Conflict of interest

The authors declare no conflict of interest.

References

1. Benfars M, Alioui A, Azalam Y, et al. (2024) Impact of ecological thermal roof insulation on the energy efficiency of conventional buildings in a semi-arid climate. *Sol Energy Sustain Dev J* 14: 78–88. https://doi.org/10.51646/jsesd.v14iSI_MSMS2E.401
2. Cavadini GB, Cook LM (2021) Green and cool roof choices integrated into rooftop solar energy modelling. *Appl Energy* 296: 117082. https://doi.org/10.1016/j.apenergy.2021.117082
3. Ong KS (2011) Temperature reduction in attic and ceiling via insulation of several passive roof designs. *Energy Convers Manag* 52: 2405–2411. https://doi.org/10.1016/j.enconman.2010.12.044
4. Abbas HM, Hussein AA (2025) Enhancing building roof insulation: A comparative examination of PCM layers integrated with and without nanoparticles. *Int J Thermofluids* 27: 101286. https://doi.org/10.1016/j.ijft.2025.101286
5. Ho ML, Yew MC, Yew MK, et al. (2024) Novel cool roofing technology system with sustainable design for attic temperature reduction. *Ain Shams Eng J* 15: 102706. https://doi.org/10.1016/j.asej.2024.102706
6. Abu-Jdayil B, Abdallah HA, Mlhem A, et al. (2022) Utilization of polyurethane foam dust in development of thermal insulation composite. *Buildings* 12: 126. https://doi.org/10.3390/buildings12020126
7. Sudirman, Anggaravidya M, Budianto E, et al. (2012) Synthesis and characterization of polyester-based nanocomposites. *Procedia Chem* 4: 107–113. https://doi.org/10.1016/j.proche.2012.06.016
8. Rana S, Fangueiro R (2016) 1–Advanced composites in aerospace engineering, In: Rana S, Fangueiro R, *Advanced Composite Materials for Aerospace Engineering*, Cambridge: Woodhead Publishing, 1–15. https://doi.org/10.1016/B978-0-08-100037-3.00001-8
9. Poorabdollah M, Beheshty MH, Atai M (2016) Investigating curing kinetics and structural relaxation phenomena of unsaturated polyester resin containing silanized silica. *J Compos Mater* 50: 2459–2467. https://doi.org/10.1177/0021998315604207
10. Gao Y, Romero P, Zhang H, et al. (2019) Unsaturated polyester resin concrete: A review. *Constr Build Mater* 228: 116709. https://doi.org/10.1016/j.conbuildmat.2019.116709
11. Tarrio-Saavedra J, López-Beceiro J, Naya S, et al. (2008) Effect of silica content on thermal stability of fumed silica/epoxy composites. *Polym Degrad Stab* 93: 2133–2137. https://doi.org/10.1016/j.polymdegradstab.2008.08.006
12. Dowou K, Nougbléga Y, Toka KA, et al. (2025) Numerical study of integrating thermal insulation local bio-sourced materials into walls and roofs for thermal comfort improvement in buildings in a tropical climate. *Constr Mater* 5: 4. https://doi.org/10.3390/constrmater5010004

13. Kumar A, Suman BM (2013) Experimental evaluation of insulation materials for walls and roofs and their impact on indoor thermal comfort under composite climate. *Build Environ* 59: 635–643. https://doi.org/10.1016/j.buildenv.2012.09.023
14. Vargas MA, Sachsenheimer K, Guthausen G (2012) In-situ investigations of the curing of a polyester resin. *Polym Test* 31: 127–135. https://doi.org/10.1016/j.polymertesting.2011.10.004
15. Guo Z, Du S, Zhang B, et al. (2005) Cure kinetics of T700/BMI prepreg used for advanced thermoset composites. *J Appl Polym Sci* 97: 2238–2241. https://doi.org/10.1002/app.21879
16. Alves FJL, Baptista AM, Marques AT (2016) 3–Metal and ceramic matrix composites in aerospace engineering, In: Rana S, Fangueiro R, *Advanced Composite Materials for Aerospace Engineering*, Cambridge: Woodhead Publishing, 59–99. https://doi.org/10.1016/B978-0-08-100037-3.00003-1
17. Nunes JP, Silva JF (2016) 5–Sandwiched composites in aerospace engineering, In: Rana S, Fangueiro R, *Advanced Composite Materials for Aerospace Engineering*, Cambridge: Woodhead Publishing, 129–174. https://doi.org/10.1016/B978-0-08-100037-3.00005-5
18. Aggarwal C, Molleti S (2024) State-of-the-art review: Effects of using cool building cladding materials on roofs. *Buildings* 14: 2257. https://doi.org/10.3390/buildings14082257
19. Chencheni A, Belkhiri S, Tarchoun AF, et al. (2024) Thermal behavior and kinetics of unsaturated polyester resin supplemented with organo-nanoclay. *RSC Adv* 14: 517–528. https://doi.org/10.1039/D3RA06076D
20. Barile C, Casavola C, De Cillis F (2019) Mechanical comparison of new composite materials for aerospace applications. *Compos Part B Eng* 162: 122–128. https://doi.org/10.1016/j.compositesb.2018.10.101
21. Abliz D, Duan Y, Steuernagel L, et al. (2013) Curing methods for advanced polymer composites: A review. *Polym Polym Compos* 21: 1–8. https://doi.org/10.1177/096739111302100602
22. Zhang Y, Huang J, Fang X, et al. (2020) Optimal roof structure with multilayer cooling function materials for building energy saving. *Int J Energy Res* 44: 1594–1606. https://doi.org/10.1002/er.4969
23. Maria M (2013) Advanced composite materials of the future in aerospace industry. *Incas Bull* 5: 139–150. https://doi.org/10.13111/2066-8201.2013.5.3.14
24. Wang X, Gao X, Zhang Z, et al. (2021) Advances in modifications and high-temperature applications of silicon carbide ceramic matrix composites in aerospace. *J Eur Ceram Soc* 41: 4671–4688. https://doi.org/10.1016/j.jeurceramsoc.2021.03.051
25. Rajak DK, Pagar DD, Menezes PL, et al. (2019) Fiber-reinforced polymer composites: Manufacturing, properties, and applications. *Polymers* 11: 1667. https://doi.org/10.3390/polym11101667
26. Ramachandran K, Bear JC, Jayaseelan DD (2025) Oxide-based ceramic matrix composites for high-temperature environments: A review. *Adv Eng Mater* 27: 2402000. https://doi.org/10.1002/adem.202402000
27. Malinverni C, Salvo M, De Zanet A, et al. (2023) Glass-ceramics for joining oxide-based ceramic matrix composites operating under direct flame exposure. *J Eur Ceram Soc* 43: 3621–3629. https://doi.org/10.1016/j.jeurceramsoc.2023.02.019
28. Talebi Z, Soltani P, Habibi N, et al. (2019) Silica aerogel/polyester blankets for efficient sound absorption in buildings. *Constr Build Mater* 220: 76–89. https://doi.org/10.1016/j.conbuildmat.2019.06.031

29. Salmoria GV, Ahrens CH, Beal VE, et al. (2009) Evaluation of post-curing and laser manufacturing parameters on properties of SOMOS 7110 resin. *Mater Des* 30: 758–763. https://doi.org/10.1016/j.matdes.2008.05.016
30. Zhang L, Zhang H, Guo J (2012) Synthesis and properties of UV-curable polyester-based waterborne polyurethane/functionalized silica composites and morphology of their nanostructured films. *Ind Eng Chem Res* 51: 8434–8441. https://doi.org/10.1021/ie3000248
31. Khankrua R, Suttiruengwong S, Hamada H (2013) Thermal and mechanical properties of biodegradable polyester/silica nanocomposites. *Energy Procedia* 34: 815–822. https://doi.org/10.1016/j.egypro.2013.06.803
32. Lekakou C, Murugesh AK, Chen YL, et al. (2008) Processability studies of silica–thermoset polymer matrix nanocomposites. *Polym Eng Sci* 48: 216–225. https://doi.org/10.1002/pen.20815
33. Abu-Jdayil B, Adi M, Al Ghaferi F, et al. (2021) Physical and thermal insulation properties of the composites based on seawater-neutralised bauxite residue. *J Hazard Mater* 403: 123723. https://doi.org/10.1016/j.jhazmat.2020.123723
34. Du S, Guo ZS, Zhang B, et al. (2004) Cure kinetics of epoxy resin used for advanced composites. *Polym Int* 53: 1343–1347. https://doi.org/10.1002/pi.1533
35. Huang C, Qian X, Yang R (2018) Thermal conductivity of polymers and polymer nanocomposites. *Mater Sci Eng R Rep* 132: 1–22. https://doi.org/10.1016/j.mser.2018.06.002
36. Han Z, Fina A (2011) Thermal conductivity of carbon nanotubes and their polymer nanocomposites: A review. *Prog Polym Sci* 36: 914–944. https://doi.org/10.1016/j.progpolymsci.2010.11.004
37. Chen H, Ginzburg VV, Yang J, et al. (2016) Thermal conductivity of polymer-based composites: Fundamentals and applications. *Prog Polym Sci* 53: 1–38. https://doi.org/10.1016/j.progpolymsci.2016.03.001
38. Burger N, Laachachi A, Ferriol M, et al. (2016) Review of thermal conductivity in composites: Mechanisms, parameters and theory. *Prog Polym Sci* 62: 1–30. https://doi.org/10.1016/j.progpolymsci.2016.05.001
39. Palacios A, Cabezón L, Navarro ME, et al. (2019) Thermal conductivity measurement techniques for characterizing thermal energy storage materials: A review. *Renew Sustain Energy Rev* 111: 224–239. https://doi.org/10.1016/j.rser.2019.03.020
40. Dai H, Wang R (2022) Methods for measuring thermal conductivity of two-dimensional materials: A review. *Nanomaterials* 12: 589. https://doi.org/10.3390/nano12040589

AIMS Press